Numerical studies of flames in wide tubes: Stability limits of curved stationary flames

O. Yu. Travnikov

Department of Physics, Uppsala University, Box 530, SE-751 21 Uppsala, Sweden

V. V. Bychkov

Department of Plasma Physics, Umeå University, SE-901 87 Umeå, Sweden

M. A. Liberman

Department of Physics, Uppsala University, Box 530, SE-751 21, Uppsala, Sweden
and P. Kapitsa Institute for Physical Problems, 117 334 Moscow, Russia

Flame dynamics in wide tubes with ideally adiabatical and slip walls is studied by means of direct numerical simulations of the complete set of hydrodynamical equations including thermal conduction, fuel diffusion, viscosity, and chemical kinetics. Stability limits of curved stationary flames in wide tubes and the hydrodynamic instability of these flames (the secondary Darrieus-Landau instability) are investigated. The stability limits found in the present numerical simulations are in a very good agreement with the previous theoretical predictions. It is obtained that close to the stability limits the secondary Darrieus-Landau instability results in an extra cusp at the flame front. It is shown that the curved flames subject to the secondary Darrieus-Landau instability propagate with velocity considerably larger than the velocity of the stationary flames.

I. INTRODUCTION

As is known [1,2], the curved shape of a premixed flame front results in increased velocity of flame propagation in comparison with the velocity of a planar flame U_f, since a curved flame has a larger surface area and consumes more fuel per unit time. Quite often a curved flame shape develops due to the hydrodynamic Darrieus-Landau (DL) instability inherent to any flame in a gaseous fuel mixture [3]. According to the linear theory of the DL instability [4], two- and three-dimensional perturbations of a planar flame front grow exponentially in time and bend the front, if the perturbation wavelength exceeds the cut-off wavelength λ_c. The instability growth rate depends on the expansion coefficient Θ of the flame defined as the ratio of the fuel density to the density of the burnt matter, which takes the values $\Theta = 5 - 10$ for laboratory flames. The cutoff wavelength λ_c is proportional to the flame thickness with a large numerical factor about 20 and larger. Perturbations of a shorter wavelength $\lambda < \lambda_c$ are suppressed by thermal conduction. If one considers development of the DL instability at a flame front propagating in a two-dimensional (2D) tube with ideally slip and adiabatical walls, then the instability occurs for a tube width exceeding the critical value $R_c = \lambda_c/2$, since the width of an ideal tube determines half of the maximal possible perturbation wavelength [5].

Outcome of the DL instability at the nonlinear stage has been a subject of long discussions starting from the original papers by Darrieus and Landau. First it was assumed that the DL instability leads to flame self-turbulization [3]. Then it was proposed that the instability results in a smooth curved stationary shape of a flame front instead of the self-turbulization [6,7]. Curved stationary flames like that shown in Fig. 1 have been observed in numerical simulations of flame dynamics in 2D tubes of moderate widths $R_c < R$

$< 3R_c$ [5,8]. The analytical theory of curved stationary flames has been developed in Ref. [9], where it was obtained that the velocity of a curved stationary flame in an ideal tube depends on the tube width R and on the expansion coefficient of the fuel Θ as

$$U_w - U_f = 4 U_m M \frac{R_c}{R}\left(1 - M\frac{R_c}{R}\right), \quad (1)$$

with the maximal velocity amplification

$$U_m = U_f \frac{\Theta}{2} \frac{(\Theta - 1)^2}{\Theta^3 + \Theta^2 + 3\Theta - 1}, \quad (2)$$

and $M = \text{Int}[R/(2R_c) + 1/2]$. The dependence of the scaled flame velocity on the inverse tube width found analytically is presented in Fig. 2 by the solid line. An important feature of the obtained formulas is existence of a maximal velocity of a curved stationary flame in a 2D configuration $(U_w)_{\max} = U_f + U_m$, that cannot be exceeded with increase of the tube width. The analytical results of Eqs. (1) and (2) are in a very good agreement with the velocity amplification found in di-
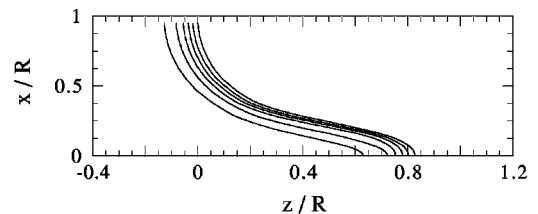
FIG. 1. The shape of a stationary curved flame with the expansion coefficient $\Theta = 8$ in a tube of width $R = 1.8R_c$. The isotherms correspond to the temperatures from 600 to 2100 K with the step 300 K.
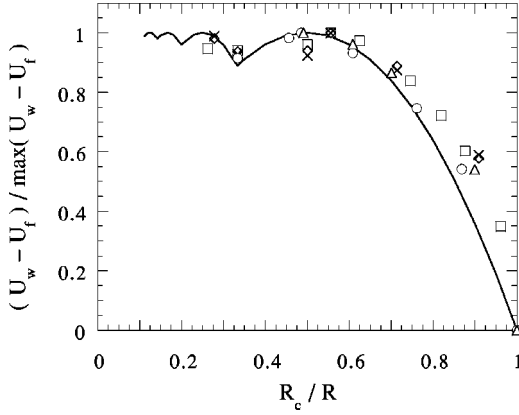
FIG. 2. Scaled velocity of a 2D curved stationary flame in an ideal tube vs the inverse tube width obtained from the analytical formula Eq. (1). The dashed line presents flame velocity for the symmetric flame shape. The markers show results of numerical simulations of Ref. [5] (triangles for $\Theta = 3$, circles for $\Theta = 5$) and of the present paper (squares for $\Theta = 6$, diamonds for $\Theta = 8$, crosses for $\Theta = 10$).

rect numerical simulations of flames in moderate tubes with ideally slip and adiabatical walls [5] shown by circles and triangles in Fig. 2.

However, curved stationary flames like that shown in Fig. 1 cannot happen in reality in very wide tubes. Indeed, as the tube width goes to infinity, the radius of curvature of the curved stationary flames becomes infinite too. In that case the stabilizing influence of the curved flame shape weakens, the flame front resembles locally a planar flame and the DL instability should occur on a new scale as discussed in Ref. [10]. This secondary DL instability presumably leads to additional wrinkling of the front and to additional increase of the flame velocity. Theoretical studies of the secondary instability have been performed mostly on the basis of a nonlinear equation for a flame front derived in Ref. [11] in the peculiar limit of small expansion coefficients $\Theta - 1 \ll 1$ (the Sivashinsky equation). These studies involved much controversy, since it was shown in [12] that curved stationary flames described by the Sivashinsky equation are linearly stable independent of the radius of curvature of the flame. The last result has been confirmed in later papers based on the Sivashinsky equation [13,14], though it obviously contradicts physical understanding of the secondary DL instability [10]. In order to avoid the contradiction it was proposed in Ref. [13] that curved stationary flames are nonlinearly unstable in wide tubes against perturbations of some finite amplitude. Still many questions remained without an answer even in scope of the idea of the nonlinear instability. Particularly, there was no indication what are the stability limits of curved stationary flames with respect to linear or nonlinear perturbations. Besides, it was claimed in Ref. [15] that it is impossible to describe correctly the secondary DL instability using the Sivashinsky equation.

A nonlinear non-stationary equation for curved flames with arbitrary large expansion coefficients has been derived recently in Ref. [16]. The complete form of the equation is rather complicated, but for a flame front $z = F(\mathbf{x}, t) - U_f t$ with thickness L_f it may be presented as

$$\frac{\Theta + 1}{2\Theta}(1 + L_f C_1 \hat{\Phi})\hat{\Phi}^{-1}\frac{1}{U_f}\frac{\partial^2 F}{\partial t^2} + (1 + L_f C_2 \hat{\Phi})\frac{\partial F}{\partial t}$$

$$+ \frac{\Theta}{2}(\nabla F)^2 + \frac{(\Theta - 1)^3}{16\Theta}\frac{\partial^2 F}{\partial t^2}[(\nabla F)^2 - (\hat{\Phi}F)^2]$$

$$- \frac{\Theta - 1}{2}(1 - L_f C_3 \hat{\Phi})\hat{\Phi}F + \Psi_t = 0, \qquad (3)$$

where the operator $\hat{\Phi}$ implies multiplication by the absolute value of the wavenumber in Fourier-space, and the numerical coefficients C_1, C_2, and C_3 may be found in scope of the linear theory of the DL instability [17]. Particularly, one has $\lambda_c = 2\pi C_3 L_f$. The simbol Ψ_t stands for nonlinear time-dependent terms of the equation. Stability investigation of curved stationary flames on the basis of Eq. (3) has shown that curved stationary flames do become unstable in sufficiently wide tubes $R > R_w$, where the critical tube width R_w characterizes the stability limits with respect to the secondary DL instability. It has been obtained that the stability limit R_w depends on the expansion coefficient of the flame being also proportional to the critical tube width of the primary DL instability R_c. Below we shall call the value R_w the second critical tube width to distinguish it from the first critical tube width R_c. It has been found in Ref. [16] that the second critical tube width is about $R_w/R_c \approx 4.2$ for flames with realistic expansion coefficients $\Theta = 5 - 10$ and this value increases as the expansion coefficient goes to unity. Taking into account the theory developed in Ref. [12] one can conclude that the second critical tube width becomes infinite $R_w \rightarrow \infty$ for $\Theta \rightarrow 1$. It was also found in Ref. [16] that stability limits of curved stationary flames do not depend on a particular form of the nonlinear time-dependent term Ψ_t in Eq. (3).

In the present paper we perform the first numerical study of the stability limits of curved stationary flames and the secondary DL instability. We investigate flame dynamics in wide tubes with ideally adiabatical and slip walls by use of direct numerical simulations of the complete set of hydrodynamical equations including thermal conduction, fuel diffusion, viscosity and chemical kinetics. The stability limits found in the present numerical simulations are in a very good agreement with the theoretical prediction of [16]. We show that the secondary DL instability for tube widths close to the stability limits results in an extra cusp at the flame front. It is also obtained that the curved flames subject to the secondary DL instability propagate with velocity considerably larger than the velocity of the stationary flames Eqs. (1) and (2).

II. BASIC EQUATIONS AND THE NUMERICAL SCHEME

We solve numerically equations of hydrodynamics and chemical kinetics. For the sake of simplicity a single irreversible reaction is admitted, so that the governing equations are the following:

$$\frac{\partial \rho}{\partial t} + \frac{\partial}{\partial x_k}(\rho u_k) = 0, \qquad (4)$$

$$\frac{\partial}{\partial t}(\rho u_i) + \frac{\partial}{\partial x_k}(\rho u_i u_k + \delta_{ik} p - \sigma_{ik}) = 0, \tag{5}$$

$$\frac{\partial}{\partial t}\left(\rho e + \tfrac{1}{2}\rho u_i u_i\right) + \frac{\partial}{\partial x_k}\left[\rho u_k(h + \tfrac{1}{2}u_i u_i) - u_i\sigma_{ik} + q k\right] = 0, \tag{6}$$

$$\frac{\partial}{\partial t}(\rho Y) + \frac{\partial}{\partial x_k}\left(\rho u_k Y - \mathrm{Le}\,\frac{\eta}{\mathrm{Pr}}\frac{\partial Y}{\partial x_k}\right) = -\exp(-E/R_g T), \tag{7}$$

where Y is the fuel mass fraction, $e = QY + C_v T$ is the internal energy and $h = QY + C_p T$ is the enthalpy. We consider a reaction of the first order with the energy release Q. The temperature dependence of the reaction rate is given by the Arrhenius law with the activation energy E and the constant of time dimension τ_R. The stress tensor and the energy diffusion vector are given by the formulas

$$\sigma_{ik} = \eta\left(\frac{\partial u_i}{\partial x_k} + \frac{\partial u_k}{\partial x_i} - \frac{2}{3}\delta_{ik}\frac{\partial u_l}{\partial x_l}\right), \tag{8}$$

$$q_k = -\frac{\eta}{\mathrm{Pr}}\left(c_p\frac{\partial T}{\partial x_k} + \mathrm{Le}\,Q\,\frac{\partial Y}{\partial x_k}\right), \tag{9}$$

where Pr is the Prandtl number and Le is the Lewis number. Since the transport properties of the fuel do not influence the nonlinear stage of the DL instability of a flame front in a tube with ideally slip and adiabatical walls [5,9], then we consider the fuel with a constant coefficient of thermal conduction, constant Prandtl number and unit Lewis number Le = 1. We take the gas mixture under consideration to be a perfect gas of molecular weight m with the equation of state $P = R_g\rho T/m$. We choose the axis z directed along the wall and the axis x in the transverse direction. An infinite length of the tube is assumed, which is achieved in simulations by an appropriate choice of the computational intervals. The boundary condition at the ideally adiabatical and slip walls of the tube of width R may be written as

$$u_x = 0, \quad u_z \neq 0, \quad \frac{\partial T}{\partial x} = 0 \quad \text{at} \quad x = 0, R. \tag{10}$$

The initial temperature of the fuel is $T_f = 300$ K and the pressure is $P_f = 10^5$ Pa. The viscosity coefficient of the fuel is $\eta = 1.82 \times 10^{-5}$ N s/m^2 with the molecular weight $m = 2.9 \times 10^{-3}$ kg/mol and the specific heat $C_p = 7R_g/2m$. The velocity of a planar stationary flame U_f is determined by the chosen values of the chemical parameters of the fuel. We are interested in dynamics of a slow flame with a velocity U_f much less than the sound speed c_s. We choose the chemical parameters of the fuel in such a way that the flame propagates in an almost isobaric regime with the Mach number $M = U_f/c_s = 0.01$. Then the main parameters of the simulations are the tube width R and the expansion coefficient Θ. For the case of isobaric flames the expansion coefficient is determined by the energy release in the reaction $\Theta = 1 + Q/(C_p T)$. When the velocity of a planar flame is known, the thickness of the flame front may be calculated by the formula $L_f = \eta/(\mathrm{Pr}\,\rho_f U_f)$. Development of the DL instability at the nonlinear stage in the case of unit Lewis number is

independent of the activation energy of the reaction [5,9]. Therefore, in all simulations we keep the same scaled value of the activation energy $E/(\Theta R_g T_f) = 7$.

The calculations consisted of the following stages similar to the calculations performed in [5]. First we ignited a planar stationary flame. To maintain the planar flame at the center of the tube close to the point $z = 0$ we imposed the following boundary conditions in the incoming flow of the fuel at $z = -Z_\infty$: $T = T_f$, $\rho = \rho_f$, $u_z = U_f$, $u_x = 0$, $Y = 1$. Similar boundary conditions for the outgoing uniform flow of the burnt matter ($z = +Z_\infty$) follow from the conservation laws of mass, momentum and energy. When a planar stationary flame is established, we impose 2D perturbations at the flame front $u_z \to u_z + \tilde{u}_z(x,z)$, where $\tilde{u}_z(x,z) = u_z(z)A_0\cos(\pi x/L)\exp(-\pi^2 z^2/L^2)$ with the initial dimensionless perturbation amplitude $A_0 = 10^{-3}$. The small perturbations grow because of the DL instability until the flame acquires a curved shape. As the curved shape of the flame develops, the flame velocity increases and the flame front pushes weak pressure waves. To avoid undesirable reflections of the pressure waves at the ends of the computational domain we used special precautions described in [5].

We carried out the numerical simulations using 2D hydrodynamic Eulerian code based on the cell-centered finite-volume scheme which was described in details previously [5,18,19]. We used a rectangular grid imposed on the finite computational domain with boundaries at $z = \pm Z_\infty$ in the longitudinal direction, with Z_∞ being $510L_f$. The size of the mesh in the vicinity of $z = 0$ was adjusted to the structure of the flame front. Along the z axis we used nonuniform grid: in the domain $-40L_f < z < 40L_f$ the grid step was constant $0.2L_f$, but outside that area the step increased gradually with factor 1.18. In the transverse direction the grid was uniform with the step R/N with $N = 20$ for narrow tubes with $R < 2R_c$ and $N = 30$ and more for wide tubes $R > 2R_c$. In order to check if the number of the grid points in the transverse direction is sufficient we performed some calculations in wide tubes with $N = 40$. However the larger number of grid points did not lead to any noticeable change in the results. On the contrary, if one takes $N = 20$ for wide tubes, then the physical results of calculations do change though not drastically, but noticeably. Particularly, for a flame with $\Theta = 8$ one obtains the stability limit $R_w \approx 3.8R_c$ for $N = 20$, while calculations with $N = 30$, 40 give $R_w \approx 4.2R_c$ in that case.

III. SIMULATION RESULTS

The main dimensionless parameters that determine dynamics of curved flames in ideal tubes are the expansion coefficient of the flame Θ and the scaled tube width R/R_c. Present numerical simulations of flame dynamics in narrow tubes $R/R_c < 1$ and tubes of moderate width $1 < R/R_c < 3$ demonstrate results similar to the previous simulations [5] and to the analytical theory [9]. We have obtained that in narrow tubes $R/R_c < 1$ the DL instability is suppressed by thermal conduction. Even if we impose initial perturbations of an appreciable amplitude, after some transitional time the perturbations vanish and the flame propagates as a planar front.

In tubes of a moderate width $1 < R/R_c < 3$ the DL instability develops and leads to a smooth curved stationary flame

front like that shown in Fig. 1. The flame front may be described as a hump directed towards the fresh fuel mixture and a cusp pointing to the products of burning. The markers (squares, diamonds and crosses) in Fig. 2 show the velocity amplification for flames with different expansion coefficients versus the inverse scaled tube width obtained in the present simulations. As one can see in Fig. 2, in agreement with the analytical theory [9] the velocity of the curved stationary flame is equal to the planar flame velocity for $R < R_c$. Increase of the tube width leads to increase of the flame velocity until it reaches a local maximum. The analytical nonlinear theory [9] predicts the local maximum for the tube width equal to the doubled first critical value $R = 2R_c$. The point of the first local velocity maximum of a curved stationary flame is also a special point in the linear theory of the DL instability [4]. According to the linear theory perturbations of a small amplitude at a planar flame front have the largest possible instability growth rate for the tube of width $R = 2R_c$. The maximal velocity amplification for curved stationary flames depends on the expansion coefficient of the fuel: the larger the expansion coefficient, the stronger the DL instability and the larger the velocity amplification. The calculated values of the maximal velocity amplification are in a very good agreement with the analytical formula Eq. (2).

Absolutely new effects of the secondary DL instability quite different from those observed in the previous simulations [5] and predicted by the theory of curved stationary flames [9] have been obtained in the present numerical simulations in the case of a sufficiently wide tube. In order to describe these effects it is convenient to use Fourier expansion of the isotherms of a flame front and to study time history of the amplitudes $F_n(t)$ of the Fourier harmonics. Since all isotherms are parallel to each other with a good accuracy, then it does not matter which of the isotherms $T = T^*$ one chooses to study. An isotherm $z = F(x,t)$ is calculated from the equation $T(x,z,t) = T^*$ and then the amplitudes $F_n(t)$ are determined as $F(x,t) = \Sigma F_n(t)\cos(n\pi x/R)$. The isotherms of a flame front with the expansion coefficient $\Theta = 8$ propagating in a tube of width $R = 4.6R_c$ are shown in Fig. 3 at different time instants after initiation of the DL instability $tU_f/R = 2.1$, 2.9, 3.5, and 7.4. The respective time history of the amplitudes of the Fourier harmonics and the velocity amplification is presented in Fig. 4. As one can see in Figs. 3(a) and 4(a), in the beginning the flame front evolves similar to the case of curved stationary flames. The first Fourier harmonic grows exponentially in time and induces growth of other harmonics due to the nonlinear interaction. As a result the flame acquires a shape similar to that shown in Fig. 1 with a well distinguished hump and cusp. The only difference of the flame in Fig. 3(a) from the stationary flame presented in Fig. 1 is a much flatter hump. Figure 3(a) corresponds to the time instant when the amplitude of the first Fourier harmonic reaches its maximum. The flat hump in Fig. 3(a) resembles locally a planar flame front, which leads to development of the secondary DL instability at the front. As one can see in Fig. 3(b) an extra cusp appears on the flat part of the front next to the center of the tube, starts growing and shifting in the direction of the hump. This leads to additional strong bending of the flame front, until a new large cusp is formed near the wall [Fig. 3(c)]. This extreme flame shape corresponds to the sharp peak in the evo-
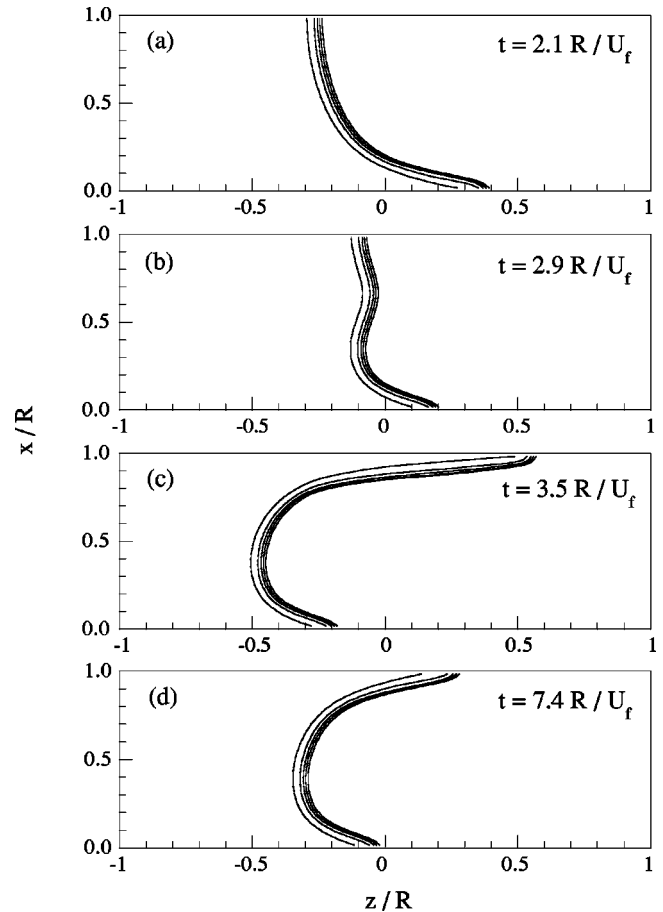
FIG. 3. Evolution of a flame front with the expansion coefficient $\Theta = 8$ in a tube of width $R = 4.6R_c$. The isotherms correspond to the temperatures from 500 to 2100 K with the step 400 K at the time instants $tU_f/R = 2.1$, 2.9, 3.5, and 7.4 [(a), (b), (c), and (d), respectively].

lution of the Fourier harmonics in Fig. 4(a). The peak of the amplitudes is accompanied by abrupt increase of the flame velocity [Fig. 4(c)]. However, this state of the flame is not stationary. As one can see in Fig. 4, the amplitude of Fourier harmonics and the flame velocity oscillate. From the point of view of flame isotherms the pulsations imply change of depth of the cusps at the flame front with the characteristic flame shape shown in Fig. 4(d). Though the pulsations on Fig. 4 are shown only up to $tU_f/R = 8$, a similar regime of pulsations have been actually observed in the simulations for thrice longer time. The secondary DL instability results in considerable growth of the second Fourier harmonic, while the first harmonic looses its dominant role. As a rule, the new extra cusp developing at the flame front has noticeably larger depth than the first one. The final shape of the flame front in Fig. 3(d) is quite different from the shape of curved stationary flames observed in [5] and described by the analytical theory [9]. First indication on the described above changes of a flame shape in wide tubes has been obtained in [20] for the case of fast nonisobaric flames with rather large Mach numbers of the incoming flow. Similar oscillations of the curved flame velocity have been also obtained in [21] in one of the calculation runs for the case of periodic boundary conditions with the period $\lambda = 4.25\lambda_c$. This period of flame structure is very close to the stability limit of curved stationary flame,
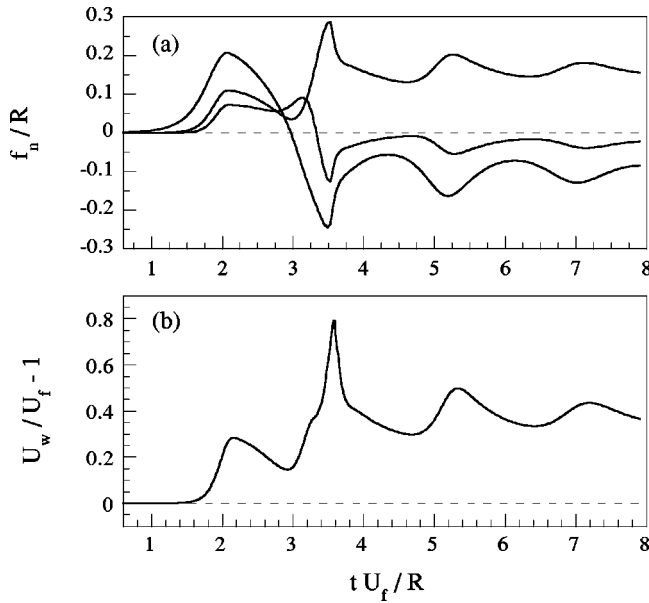
FIG. 4. The time history of the scaled amplitude of the first three Fourier harmonics [(a), curves 1, 2, 3] and the scaled flame velocity (b) in a tube of width $R = 4.6R_c$. The expansion coefficient of the flame is $\Theta = 8$.

found in the present paper. The small deviation of the results [21] from our results may be explained by somewhat lower calculation accuracy of the mentioned simulations, which leads to smaller stability limits (see discussion at the end of the previous section). One more comment should be given concerning Figs. 3 and 5. The adiabatic boundary condition at the walls requires that flame isotherms should touch the walls at a right angle, which is not obvious for some of the isotherms at the figures. However, the ''smashed'' right angle for these isotherms results from smoothing of the curves on the figures and has nothing to do with numerical accuracy of the calculations.

However, the described above scenario of the secondary DL instability is not the only possible one. For example, in the case of a flame in a tube of the same width $R = 4.6R_c$ but with smaller expansion coefficient $\Theta = 6$ (see Figs. 5 and 6) the extra cusp arising near the center of a tube [Fig. 5(b)] shifts not in the direction of the hump as in the previous case but to the cusp. This causes additional stretching of the cusp while the front retains its original shape [Fig. 5(c)]. This case is also characterized by rapid increase both of the amplitudes of Fourier harmonics [Fig. 6(a)] and of the velocity amplification [Fig. 6(b)]. But after short time the flame front also acquires its new shape [Fig. 5(d)] similar to that described above [Fig. 3(d)]. It is interesting to note, that in the last case the final flame shape is practically stationary.

Another important point is that the new shape of the flame front leads to considerable increase of the flame velocity in comparison with the velocity of curved stationary flames described in [5,9]. The velocity amplification for flames with the expansion coefficient $\Theta = 8$ versus the tube width is shown in Fig. 7 by diamonds. Careful investigation of flame dynamics in tubes of different widths for a fixed expansion coefficient of the fuel $\Theta = 8$ shows that the additional velocity amplification and the described changes in the flame shape take place for the tube width larger than some critical
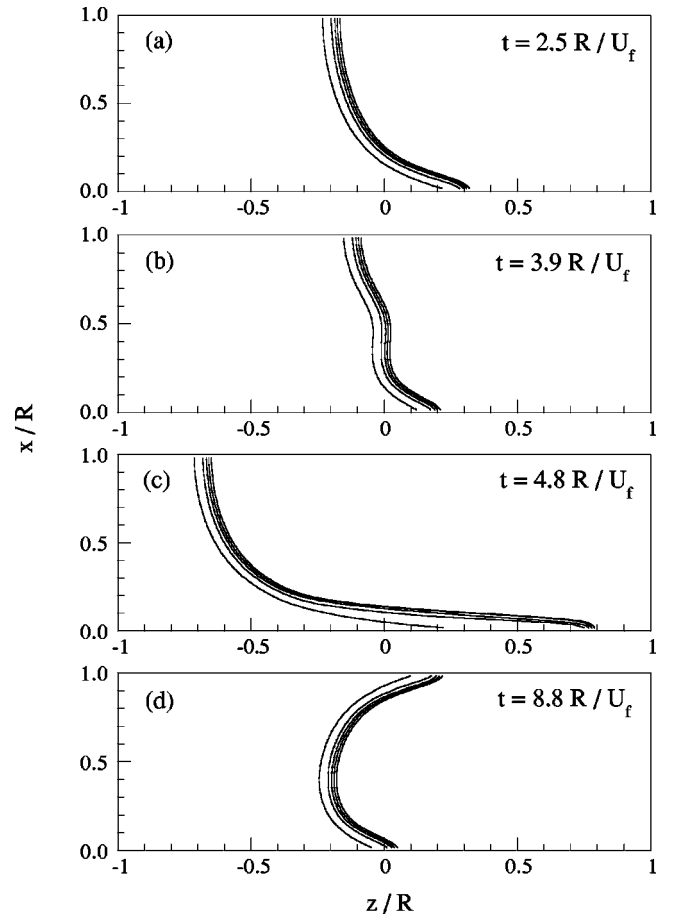
FIG. 5. Evolution of a flame front with the expansion coefficient $\Theta = 6$ in a tube of width $R = 4.6R_c$. The isotherms correspond to the temperatures from 500 to 2100 K with the step 400 K at the time instants $tU_f/R = 2.5$, 3.9, 4.8, and 8.8 [(a), (b), (c), and (d), respectively].

value $R > 4.2R_c$. The critical value $R_w = 4.2R_c$ represents the stability limit of a curved stationary flame with the expansion coefficient $\Theta = 8$. Similar dependence of the velocity amplification on the tube width has been obtained for flames with other expansion coefficients. Particularly, the additional velocity amplification has been observed for flames with the expansion coefficient $\Theta = 10$ for a tube width $R > R_w = 4.3R_c$ (shown by circles in Fig. 7) and for flames with the expansion coefficient $\Theta = 6$ for a tube width $R > R_w = 4.4R_c$ (shown by triangles in Fig. 7). The stability limits of curved stationary flames found numerically in the present simulations are compared to the theoretical predictions of [16] in Fig. 8. As one can see in Fig. 8 the numerical and theoretical results are in a very good agreement.

IV. DISCUSSION

Simulations of the present paper demonstrate that curved stationary flames in tubes with ideally slip and adiabatical walls become unstable as soon as the tube width exceeds certain critical value R_w. For flames with realistic expansion coefficients the second critical tube width R_w is approximately four times larger than the first critical tube width R_c, for which the DL instability overcomes the stabilizing influence of thermal conduction: $R_w/R_c = 4.2 - 4.4$. The obtained
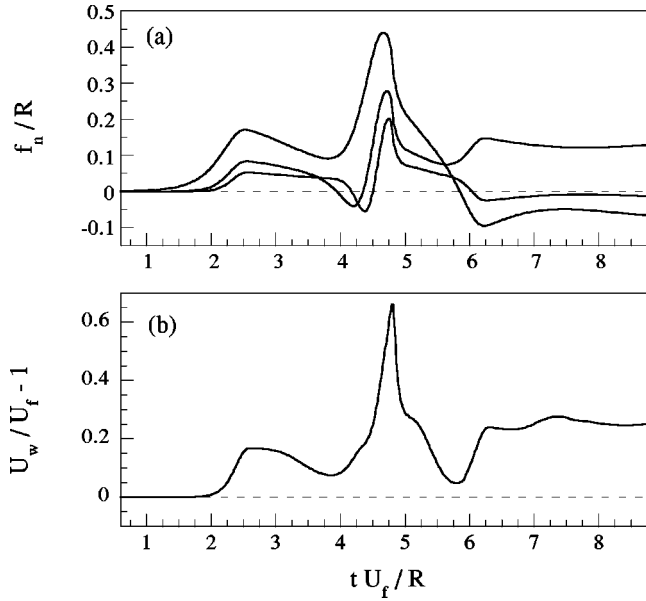
FIG. 6. The time history of the scaled amplitude of the first three Fourier harmonics [(a), curves 1, 2, 3] and the scaled flame velocity (b) in a tube of width $R=4.6R_c$. The expansion coefficient of the flame is $\Theta=6$.

stability limits of the curved stationary flames are in a very good agreement with the theoretical predictions $R_w/R_c=4.2-4.3$ [16]. In wider tubes the secondary DL instability takes place, which is the next step in the development of the instability at a planar flame after the primary DL instability. While the primary instability results in curved stationary flames for the tube width $R_c<R<R_w$, the secondary one leads to an extra cusp at the flame front for wider tubes $R>R_w$ and sometimes to pulsations of the flame shape. The primary instability amplifies the velocity of a flame front with a realistic expansion coefficient by the factor about $U_w/U_f=1.2-1.35$ determined by Eq. (2). Taking into account physical similarity between the primary and secondary instabilities one should expect that the secondary instability leads to amplification of the flame velocity by the factor
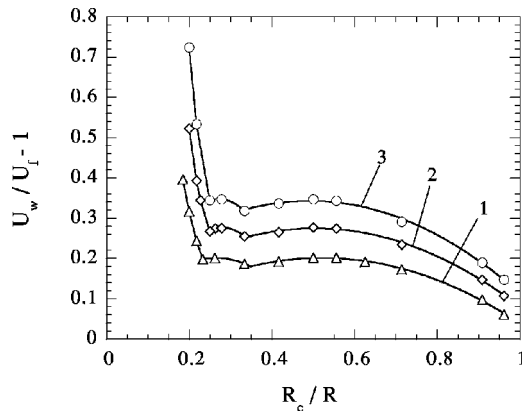
FIG. 7. The scaled velocity of a curved stationary flame as a function of the inverse tube width for different expansion coefficients: (1) $\Theta=6$; (2) 8; (3) 10. The markers show the results of 2D simulations, the solid lines present the best parabolic approximation.
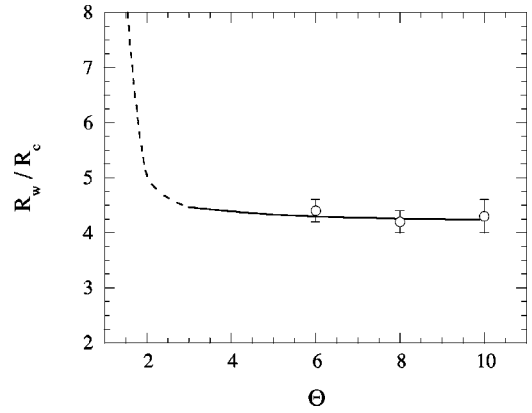
FIG. 8. The scaled second critical tube width as a function of the expansion coefficient. Markers represent the results of the numerical simulations, solid line shows analytical results from Ref. [16]. The dashed line shows the estimation taking into account the theory from Ref. [12].

$$U_w/U_f=\left[1+\frac{\Theta}{2}\frac{(\Theta-1)^2}{\Theta^3+\Theta^2+3\Theta-1}\right]^2 \quad (11)$$

for the tube widths $R_w<R<R_w^2/R_c$. According to the estimate Eq. (11) the characteristic amplification of the flame velocity due to the secondary DL instability is $U_w/U_f=1.6$ for $\Theta=6$, $U_w/U_f=1.76$ for $\Theta=8$ and $U_w/U_f=1.85$ for $\Theta=10$. The respective numerical results for the velocity amplification are $U_w/U_f=1.4;1.5;1.7$ for $\Theta=6;8;10$, which is somewhat smaller than the estimate Eq. (11). However, the growth of flame velocity with the tube width obtained in numerical simulations is not saturated yet. For wider tubes one should expect even larger flame velocities. Thus according to the theoretical predictions and to the numerical results flame velocity is amplified about twice for flames with realistic expansion coefficients in tubes of widths $4R_c<R<16R_c$.

For wider tubes further development of the DL instability is expected leading to a fractal flame structure similar to that observed in the experiments [22]. In a certain sense one can interpret the fractal structure as spontaneous turbulization of the flame front. A fractal structure of a flame front implies cascades of humps and cusps of different sizes imposed one on another. The fractal flame structure may be described tentatively in the following way. Assuming that every step of the cascade amplifies the size of the humps and the flame velocity by the factors b and β, respectively, one finds that the velocity of the fractal flame depends on the largest possible length scale characterizing flame dynamics as [23]

$$U_w\propto(R_{\max}/R_{\min})^d, \quad (12)$$

where $d=\ln\beta/\ln b$ is the excess of the fractal dimension over the embedding dimension. Evaluating the factor β for 2D fractal flames with the help of Eq. (2),

$$\beta_{2D}=1+\frac{\Theta}{2}\frac{(\Theta-1)^2}{\Theta^3+\Theta^2+3\Theta-1}, \quad (13)$$

and the factor b as $b_{2D}=R_w/R_c$ we find the estimate for the fractal excess d_{2D} of 2D flames as shown in Fig. 9. The solid
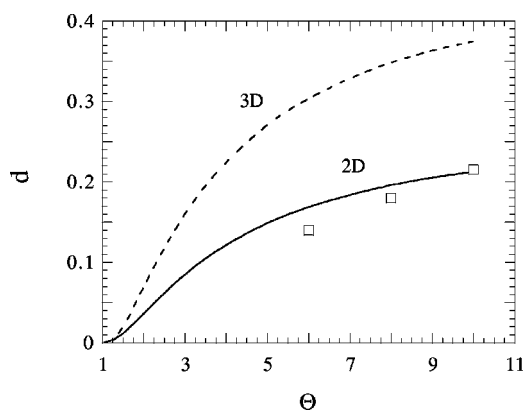
FIG. 9. Excess of the fractal dimension over the embedding dimension as a function of the expansion coefficient. The solid line presents the evaluation on the basis of the analytical theory [9,16] and the markers show the evaluation using the present numerical results for the 2D case. The dashed line is the estimation for the 3D case.

line in Fig. 9 presents the evaluation of the fractal excess made on the basis of the analytical theory [9,16], while the markers show the evaluation performed by use of the numerical results of the present paper. As one can see, both evaluations are rather close to each other predicting the fractal dimension 1.18–1.22 for 2D flames with realistic expansion coefficients. The fractal dimension depends on the expansion coefficient of the flame increasing with increase of the fuel expansion. In the case of 3D flames the DL instability is stronger at the nonlinear stage and a larger fractal excess over the embedding dimension is expected. The velocity amplification for 3D flames on every step of the fractal structure is about twice larger than in the 2D case [24,19,25]

$$\beta_{3D} = 1 + \frac{\Theta(\Theta-1)^2}{\Theta^3 + \Theta^2 + 3\Theta - 1}, \qquad (14)$$

There are no results on stability limits of 3D curved stationary flames yet, therefore the only estimate for the factor b_{3D} available so far comes from the theory of 2D flames. Adopting the estimate $b_{3D} \approx 4$ in the 3D case we obtain the evaluation for the fractal excess of a 3D flame front shown in Fig. 9 by the dashed line. The estimated fractal dimension depends also on the expansion coefficient of the flame predicting the values 2.3–2.35 for flames with realistic expansion coefficients. Though the last estimates are very tentative, they agree well with the experimentally measured values 2.33 of the fractal dimension for spherically expanding laboratory flames [22].

[1] Ya. B. Zeldovich, G. I. Barenblatt, V. B. Librovich, G. M. Makhviladze, *The Mathematical Theory of Combustion and Explosion* (Consultants Bureau, New York, 1985).

[2] F. A. Williams, *Combustion Theory* (Benjamin/Cummings, Menlo Park, CA 1985), 2nd ed.

[3] L. D. Landau and E. M. Lifshitz, *Fluid Mechanics* (Pergamon, Oxford, 1987).

[4] P. Pelce and P. Clavin, J. Fluid Mech. **124**, 210 (1982).

[5] V. V. Bychkov, S. M. Golberg, M. A. Liberman, and L.-E. Eriksson, Phys. Rev. E **54**, 3713 (1996).

[6] G. H. Markstein, *Nonsteady Flame Propagation* (Pergamon Press, Oxford, 1964).

[7] Ya. B. Zeldovich, Prikl. Mekh. Tekh. Fiz. **1**, 102 (1966).

[8] B. Denet and P. Haldenwang, Combust. Sci. Technol. **104**, 143 (1995).

[9] V. V. Bychkov, Phys. Fluids **10**, 2091 (1998).

[10] Ya. B. Zeldovich, A. G. Istratov, N. I. Kidin, and V. B. Librovich, Combust. Sci. Technol. **24**, 1 (1980).

[11] G. I. Sivashinsky, Acta Astronaut. **4**, 1177 (1977).

[12] O. Thual, U. Frish, and M. Henon, J. Phys. (France) **46**, 1485 (1985).

[13] G. Joulin, J. Phys. (France) **50**, 1069 (1989).

[14] Z. Olami, B. Galanti, O. Kupervasser, and I. Procaccia, Phys. Rev. E **55**, 2649 (1997).

[15] S. I. Blinnikov and P. V. Sasorov, Phys. Rev. E **53**, 4827 (1996).

[16] V. V. Bychkov, K. A. Kovalev, and M. A. Liberman, Phys. Rev. E **60**, 2897 (1999).

[17] G. Searby, D. Rochwerger, J. Fluid Mech. **231**, 529 (1991).

[18] L.-E. Eriksson, Comput. Methods Appl. Mech. Eng. **64**, 95 (1987).

[19] V. V. Bychkov, S. M. Golberg, M. A. Liberman, A. I. Kleev, and L.-E. Eriksson, Combust. Sci. Technol. **129**, 217 (1997).

[20] O. Yu. Travnikov, V. V. Bychkov, and M. A. Liberman, Phys. Fluids **11**, 2657 (1999).

[21] B. Denet and J. Bonino, Combust. Sci. Technol. **99**, 235 (1994).

[22] Y. I. Gostintsev, A. G. Istratov, and Y. V. Shulenin, Combust. Explos. Shock Waves **24**, 70 (1988).

[23] V. V. Bychkov and M. A. Liberman, Phys. Rev. Lett. **76**, 2814 (1996).

[24] V. V. Bychkov, A. I. Kleev, M. A. Liberman, and S. M. Golberg, Phys. Rev. E **56**, R36 (1997).

[25] V. V. Bychkov and A. I. Kleev, Phys. Fluids **11**, 1890 (1999).